

# Rejuvenation and memory in model spin glasses in three and four dimensions

S. Jiménez,<sup>1,2</sup> V. Martín-Mayor,<sup>3,2</sup> and S. Pérez-Gaviro<sup>4,2</sup>

<sup>1</sup>Dipartimento di Fisica, INFN and SMC, U. di Roma La Sapienza, P.le A. Moro 2, Roma I-00185, Italy

<sup>2</sup>Instituto de Biocomputación y Física de Sistemas Complejos (BIFI), Corona de Aragón 42, Zaragoza 50009, Spain

<sup>3</sup>Departamento de Física Teórica I, Facultad de Ciencias Físicas, Universidad Complutense, 28040 Madrid, Spain

<sup>4</sup>Departamento de Física Teórica, Universidad de Zaragoza, Zaragoza 50009, Spain

(Received 24 February 2005; published 15 August 2005)

We numerically study aging for the Edwards-Anderson model in three and four dimensions using different temperature-change protocols. In  $D=3$ , time scales a thousand times larger than in previous work are reached with the Spin Update Engine (SUE) machine. Deviations from cumulative aging are observed in the nonmonotonic time behavior of the coherence length. Memory and rejuvenation effects are found in a temperature-cycle protocol, revealed by vanishing effective waiting times. Similar effects are reported for the  $D=3$  site-diluted ferromagnetic Ising model (without chaos). However, rejuvenation is reduced if off-equilibrium corrections to the fluctuation-dissipation theorem are considered. Memory and rejuvenation are quantitatively describable in terms of the growth regime of the spin-glass coherence length.

DOI: [10.1103/PhysRevB.72.054417](https://doi.org/10.1103/PhysRevB.72.054417)

PACS number(s): 75.10.Nr, 05.70.Ln, 75.40.Mg

## I. INTRODUCTION

Nowadays the arena for comparisons between theory and experiments in spin-glass physics<sup>1</sup> is out-of-equilibrium dynamics.<sup>2</sup> Spin glasses *age*,<sup>3</sup> as shown by the thermoremanent magnetization: consider a spin glass that has spent a time  $t_w$  below its glass temperature  $T_c$  in the presence of a magnetic field. Let  $t$  be the time elapsed since the magnetic field was switched off. The magnetization decays as a function of  $t/t_w^\mu$ , even for  $t_w \sim 1$  day. The exponent  $\mu$  could be 1 (*full aging*),<sup>4</sup> although there are recent experimental claims for  $\mu$  being smaller than 1 (*subaging*).<sup>5</sup> A somehow complementary experiment consists in keeping the system for  $t_w$  below its glass temperature. Then, a magnetic field is switched on and the so-called zero-field-cooled (ZFC) magnetization is recorded while it grows.<sup>6</sup> Full aging can be also observed in the ac magnetic susceptibility  $\chi(\omega, t_w)$  which, for a fixed  $\omega$ , decreases as  $t_w$  grows. This time decay can be rescaled as a  $\omega$ -independent function of  $\omega t_w$ ,<sup>2</sup> although, experimentally, one is restricted to the range  $\omega t_w > 1$ .

*Memory and rejuvenation*<sup>7,8</sup> are sophisticated manifestations of aging in experiments where the temperature is not kept constant. Rejuvenation arises when changing temperature from  $T_1$  to  $T_2$  ( $T_1$  and  $T_2$  smaller than the critical temperature  $T_c$ ) a system that has spent some time at  $T_1$ , so that  $\chi(\omega, t_w)$  barely depends on  $t_w$ . Just after the  $T_1 \rightarrow T_2$  change, aging restarts. The imaginary part of the susceptibility suddenly grows then relaxes. The  $t_w$  dependency of  $\chi''(\omega, t_w)$  gets stronger, as for a *younger* system. Rejuvenation means that the relaxation of  $\chi''(\omega, t_w)$  is very similar to the one of a system just quenched from  $T > T_c$  to  $T_2$ . Sometimes it is said that the relaxation is identical to the one of a system instantaneously quenched to  $T_2$  from infinite temperature (in Sec. III B, below, we elaborate on the different meaning of *instantaneous temperature quench* in a experiment and in a computer simulation). If the susceptibility just after the quench to  $T_2$  rises *above* the final value it had at  $T_1$ , one speaks of *strong rejuvenation*.<sup>9</sup> On the other hand, when the system is

put back at temperature  $T_1$ ,  $\chi''(\omega, t_w)$  continues its relaxation where it left it just before the temperature change (*memory effect*). These effects can also be observed in the real part of the susceptibility (see, e.g., Fig. 1 of Ref. 10), although rejuvenation is very diminished as compared with the imaginary part. With the sophisticated *dip-experiment* temperature-change protocol,<sup>7</sup> memory and rejuvenation are truly spectacular.

Memory and rejuvenation have been found in systems quite different from spin glasses (see, however, Ref. 11). Examples are structural glasses,<sup>12</sup> polymers [Poly methyl methacrylate (Refs. 13 and 14)], and systems not particularly glassy (or not widely recognized as such), like colossal magnetoresistance oxides.<sup>15</sup> Moreover, a disordered ferromagnetic alloy,<sup>16</sup> becoming spin glass at lower temperatures, has shown rejuvenation and memory, through the dip-experiment protocol (although in this case memory could be easily erased by lowering the temperature). Spin glasses display the quantitatively stronger effects, but it is unlikely that the physical mechanisms underlying memory and rejuvenation are specific of spin glasses.

The above definitions for memory and rejuvenation need qualification. Under very small temperature changes<sup>17</sup> [say  $(T_1 - T_2)/T_1 < 5 \times 10^{-3}$ ] the behavior of the spin glass is rather smooth. On the other hand, sharp memory and rejuvenation can be observed<sup>18</sup> for  $(T_1 - T_2)/T_1 \sim 0.07$ . The cross-over from small to drastic effects is rationalized using *effective isothermal waiting times*.<sup>17,19</sup> Consider the simplest temperature change protocol: a system is aged for time  $t_w$  at temperature  $T_1$ , then its temperature is suddenly shifted from  $T_1$  to  $T_2$ . After the shift, the ZFC magnetization is measured. The effective time  $t_{T_2}^{\text{eff, shift}}$  is the age of the isothermally aged system at temperature  $T_2$ , whose ZFC magnetization<sup>20</sup> is most similar to the one of the temperature-shifted system (the two relaxations are not identical<sup>17</sup>). Rejuvenation arises when  $t_{T_2}^{\text{eff, shift}}/t_w$  is below experimental resolution.

Similarly, one can define<sup>19</sup> an effective time for the temperature cycle protocol  $T_1 \rightarrow T_2 \rightarrow T_1$ :<sup>21</sup> one keeps the system

a time  $t_w$  at  $T_1$ , then shifts the temperature to  $T_2$ , waits a time  $t_2 \sim 20t_w$ , shifts back the temperature to  $T_1$ , switches on a magnetic field, and then records the ZFC magnetization. The effective time  $t_{T_1}^{\text{eff,cycle}}$  is obtained by looking to the system aged at temperature  $T_1$  for a time  $t_w + t_{T_1}^{\text{eff,cycle}}$  whose ZFC magnetization is most similar to the one of the temperature-cycled system. One has memory, as we defined it above, when  $t_{T_1}^{\text{eff,cycle}}/t_2$  gets below experimental resolution. A large variety of spin-glass experiments find<sup>5,19</sup> for  $T_1 > T_2$ ,

$$\frac{t_{T_1}^{\text{eff,cycle}}}{t_w} = \exp\left[-\frac{T_1 - T_2}{x_0 T_2}\right], \quad (1)$$

with<sup>22</sup>

$$x_0 \sim 10^{-2}. \quad (2)$$

The theoretical investigation of these phenomena is less advanced than its experimental counterpart. Memory and rejuvenation can be recovered in the dynamics of abstract energy-landscape models.<sup>23</sup> However, one wants to reproduce these phenomena in the Langevin dynamics for the standard spin-glass model, the Edwards-Anderson (EA) model.<sup>1</sup> This dynamics for the EA model can only be investigated by Monte Carlo simulation. Yet, difficulties have arisen in numerical investigation of memory and rejuvenation.<sup>9,24–27</sup> Furthermore, the progress achieved regards temperature-shift and temperature-cycle experiments. The dip-experiment protocol remains still as too complicated to be analyzed theoretically.

Experiments where  $(T_2 - T_1)/T_1$  is very small can be accounted for by the *cumulative aging* scenario,<sup>17,19</sup> consisting in the three following hypotheses:

(i) Aging is ruled by the growth of a coherence length,<sup>28</sup> signaling the building of a spin-glass order. For isothermal aging, this length is named  $\xi_T(t)$ ,  $t$  being the total time spent in the glass phase. This isothermal growth law has been studied in experiments<sup>19</sup> and simulations,<sup>29,30</sup> although the measured  $\xi_T(t)$  grows by a small factor in both cases. Numerically, a power law,

$$\xi_T(t) = A_T t^{z(T)}, \quad z(T) = z_c \frac{T}{T_c}, \quad (3)$$

fairly fits the data. However, more complicated rules have been used.<sup>5,17–19</sup>

(ii) The coherence length always grows with time. It behaves continuously upon temperature changes.

(iii) Effective times follow from the *isothermal* growth of the coherence length. Consider a temperature shift after aging for time  $t_w$  at  $T_1$ . One has

$$\xi_{T_1}(t_w) = \xi_{T_2}(t_{T_2}^{\text{eff,shift}}). \quad (4)$$

A time  $t$  after the shift, the coherence length is

$$\xi^{\text{shift}}(t) = \xi_{T_2}(t + t_{T_2}^{\text{eff,shift}}). \quad (5)$$

Similar reasoning is used in the analysis of more complicated temperature-change protocols.

Equation (4) is used in an indirect way, both in the analysis of simulations<sup>9,27</sup> and experiments.<sup>17–19</sup> Relations such as

Eq. (3), obtained in a different experiment, are used to convert the measured effective times into length scales and vice versa. It is difficult to find in the literature *direct* data on the behavior of the coherence length upon temperature changes. A nice exception is the simulations of Ref. 24 where Eq. (5) was directly checked. Those simulations spanned  $10^5$  Monte Carlo steps (MCSs). For comparison with experiments, recall that  $1 \text{ MCS} \sim 1 \text{ ps}$ .

Memory and rejuvenation appear as hardly compatible with the cumulative aging. Experiments show<sup>17</sup> that  $\xi_{T_1}(t_w) < \xi_{T_2}(t_{T_2}^{\text{eff,shift}})$  when the measured effective times are converted in length scales, both for  $T_2 > T_1$  and  $T_1 < T_2$ , in contradiction with Eq. (4).

Two theoretical scenarios are currently being considered to account for memory and rejuvenation. Rejuvenation was interpreted in terms of temperature chaos,<sup>31</sup> namely extreme sensitivity of *equilibrium* states in the glass phase to small temperature changes. An overlap-length  $l_0(T_1, T_2)$  is postulated to exist. Features at a scale smaller than  $l_0$  are unaffected by a temperature change  $T_1 \rightarrow T_2$  while at larger scales the system is completely reorganized. Rejuvenation is then attributed to large length scales and strong rejuvenation requires small  $l_0$ . The ghost-domain scenario (see Ref. 18 for a recent account) allows us to reproduce memory in the chaos scenario. The other scenario<sup>32</sup> is closer in spirit to cumulative aging. Rejuvenation after a negative temperature shift would arise from the so-called fast modes involving length scales smaller than  $\xi_{T_1}(t_w)$ , that were equilibrated at  $T_1$  but fall out of equilibrium at  $T_2$ . Memory would arise from time and length scales separation: back to temperature  $T_1$ , fast modes re-equilibrate very fast so that aging continues from the previous  $T_1$  state.

However, when it comes to actual calculations, it turns out that no convincing memory and rejuvenation has been found in computer simulations of three-dimensional (3D) spin-glass models, either with a two-temperature<sup>9,24,26,27</sup> or with a dip-experiment protocol.<sup>25</sup> When the behavior of the coherence length is followed for times up to  $10^5$  MCSs,<sup>24</sup> Eqs. (4) and (5) are fulfilled even for  $(T_1 - T_2)/T_2 \approx \pm 0.33$ . Consistent with this finding, when the temperature cycle protocol is analyzed in the EA model,<sup>27,33</sup> the  $x_0$  in Eq. (1) turns out to be of order 1 rather than of order  $10^{-2}$ . Should  $x_0$  not decrease significantly for larger times, the whole low-temperature phase of the EA model could be accounted for by cumulative aging (i.e., the low-temperature phase would not be a spin-glass phase).

This contradiction with experiments is puzzling. It could be indicating that the EA model lacks some crucial ingredient<sup>25</sup> (maybe long-ranged dipolar interactions?). Or maybe memory and rejuvenation involve time and length scales inaccessible to present-day simulations. Indeed, experiments are performed on a time scale which is about  $10^8$  times longer than typical simulations. Yet, experimentally,<sup>19</sup> there are around  $\sim 10^5$  spins in a coherent cluster [hence  $\xi_T(t_w) \sim 40$  lattice spacings], while simulations achieve (see below)  $\xi_T(t_w) \sim 10$  lattice spacings. When length scales are confronted, the differences with experimental conditions do not seem so dramatic.

As for higher space dimensions, a simulation<sup>26</sup> of the temperature cycle protocol for the 4D EA model, yielded strong

rejuvenation (as defined in Ref. 9). Yet, results in full agreement with cumulative aging, Eq. (4), were reported for  $(T_1 - T_2)/T_2 \approx \pm 0.125$  (the simulation time was smaller than  $10^4$  MCSs). In the Migdal-Kadanof lattice,<sup>34</sup> where rather larger times can be simulated, rejuvenation was found for  $(T_1 - T_2)/T_1 \sim 0.1$ , suggesting that  $x_0$  in Eq. (1) does depend on the age of the system.

In this work, we report simulations of a 3D (made with the SUE machine<sup>35</sup>) and a 4D EA model with *binary* (rather than *Gaussian*<sup>24–26,34</sup>) couplings. Our 3D simulations are three orders of magnitude longer than previous ones. We use real replicas<sup>29</sup> to study the coherence length, that is directly calculated (not inferred from effective times), through the temperature changes. In a temperature-cycle protocol, clear memory and rejuvenation effects are found for large values of  $(T_2 - T_1)T_1$  both in three and in four dimensions (Secs. III A and III B). We also observe strong rejuvenation (in the sense of Ref. 9), but only if we neglect corrections to the fluctuation-dissipation theorem.<sup>36</sup> The coherence length is shown to *decrease* upon some temperature changes, in contradiction with cumulative aging. Moreover, a value  $t_{T_1}^{\text{eff,cycle}}$  compatible with zero can be obtained for  $T_1 = 0.9T_c$  and  $T_2 = 0.4T_c$ , which is to be expected in view of Eqs. (1) and (2) (Secs. III B and III C). Furthermore, we will show that the two-times dependency of the time correlation function can be accounted for with surprising accuracy by the coherence length at the two relevant times, both for isothermal aging and for temperature-shift protocols (Sec. III D). We perform exactly the same calculations for the 3D *ferromagnetic* site-diluted Ising model<sup>37</sup> (where, in the absence of frustration, chaos is absent), obtaining very similar results. Although temperature chaos is probably present in models for spin glasses,<sup>34,38</sup> our results in the site-diluted *ferromagnetic* Ising model suggest that it plays no role in producing memory and rejuvenation. This was maybe to be expected, since memory and rejuvenation is being found experimentally in materials where chaos in temperature seems to be absent or where a thermodynamic glass transition has never been found.<sup>12–14</sup> Unfortunately, we have made no progress<sup>39</sup> in the analysis of the dip-experiment protocol.

## II. MODELS AND SIMULATIONS

Specifically, we consider Ising variables,  $\sigma_i = \pm 1$ , occupying the nodes of a (hyper)cubic lattice in three and four dimensions with nearest-neighbor, quenched disordered interactions. We report results for the spin glass with random  $\pm 1$  couplings and the 3D site-diluted Ising ferromagnet<sup>37</sup> (spins are lacking with probability  $1-p$ ). We evolve the system using a sequential, local heat-bath dynamics. Our time unit (1 MCS  $\sim$  1 ps) is a full-lattice update. For the spin glass we studied the lattice size  $L=60$  in three dimensions (mostly in SUE), and  $L=20$  for four dimensions (on PC clusters) with some tests in  $L=30$  finding no differences. For the site-diluted model we studied  $L=100$ . The number of disorder realizations vary within 16 and 240.

In the following, we will call a *direct quench* to the procedure of placing a fully disordered system (infinite tempera-

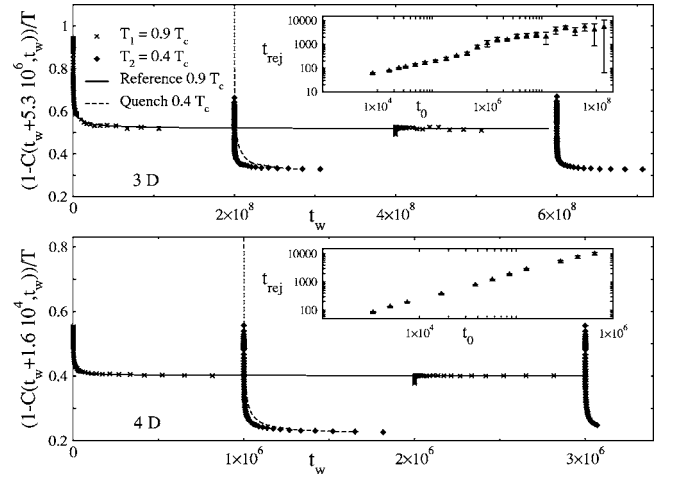


FIG. 1. Top: Naive  $\chi(\omega = 2\pi/t_0, t_w)$ ,  $t_0 = 5.3 \times 10^6$  for the 3D EA model vs time. The  $T$  cycle is  $T_1 \rightarrow T_2 \rightarrow T_1 \rightarrow T_2$ , each step lasting  $t_s = 2 \times 10^8$ . The full line is a reference run at  $0.9T_c$ . The inset shows the rejuvenation time (see text) vs  $t_0$ . The dashed line is a direct quench to  $T_2$ . Bottom: as top part for  $D=4$ ,  $t_0 = 1.6 \times 10^4$  and  $t_s = 10^6$ .

ture) instantaneously at the working temperature. This corresponds to an infinite quenching rate.

The fluctuation-dissipation theorem (FDT) relates the autocorrelation function in zero magnetic field,

$$C(t_w, t_w + t_0) = \frac{1}{V} \sum_i \langle \sigma_i(t_w) \sigma_i(t_w + t_0) \rangle, \quad (6)$$

to the real part of the susceptibility:  $\chi(\omega = 2\pi/t_0, t_w) \approx [1 - C(t_w, t_w + t_0)]/T$ . Yet, off equilibrium, FDT needs to be generalized replacing  $T$  by  $T/X[C]$  ( $X[C]$  is a smooth function<sup>36</sup> of  $C(t_w, t_w + t_0)$ ). Hence one assumes<sup>24–26,34</sup> to be in pseudoequilibrium regime ( $\omega t_w \gg 1$  thus  $X[C] = 1$ ), which is not always true. We also obtain *spatial* information from the correlation function of the overlap field,  $q_i(t) = \sigma_i^{(1)}(t) \sigma_i^{(2)}(t)$ , built from two independently evolving systems with the same couplings, at the same temperature:

$$C_4(r, t_w) = \frac{1}{V} \sum_i \langle q_i(t_w) q_{i+r}(t_w) \rangle. \quad (7)$$

## III. RESULTS

### A. Strong rejuvenation?

In Fig. 1 is shown the time evolution of the naive  $\chi(\omega, t_w)$  (i.e.,  $[1 - C(t_w, t_w + t_0)]/T$ ) for the EA model in three dimensions (top) and four dimensions (bottom) for a (double) temperature cycle:  $T_1 \rightarrow T_2 \rightarrow T_1 \rightarrow T_2$  ( $T_1 = 0.9T_c$ ,  $T_2 = 0.4T_c$ ). In three dimensions the system spends  $t_s = 2 \times 10^8$  MCSs at each temperature (1000 times longer than previous works), while in four dimensions  $t_s = 10^6$  MCSs. The results of a reference run, with temperature fixed to  $T_1$ , are also shown (continuous line). When the temperature drops to  $T_2$ ,  $\chi(\omega, t_w)$  increases over the reference curve and starts a new relaxation (*strong*

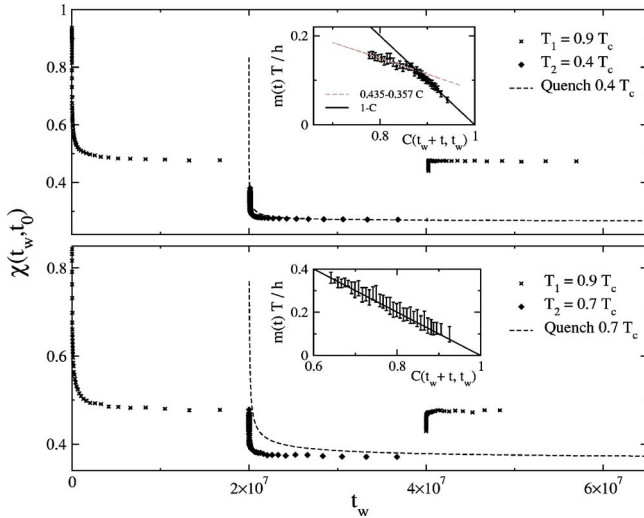


FIG. 2. (Color online) Top: As Fig. 1 for  $t_0=4.3 \times 10^5$  and  $t_s = 2 \times 10^7$  but correcting FDT violations. Inset: Off-equilibrium fluctuation dissipation relation (see text). Data can be nicely fitted to two straight lines. Bottom: As in top part for  $T_2=0.7T_c$ . Only the pseudoequilibrium regime is explored in this case (inset).

rejuvenation<sup>9</sup>). When temperature is back to  $T_1$ ,  $\chi(\omega, t_w)$  catches the reference run almost instantaneously (*memory*). We call  $t_{\text{rej}}$  the time that the rejuvenated  $\chi(\omega, t_w)$  is above the reference run (see insets in Fig. 1), that is found to grow consistently with  $t_0$  (much faster in four dimensions). It is then conceivable that an effect of macroscopic time duration could be observed (experiments explore  $t_0 \sim 10^{13}$  MCSs). However, especially in three dimensions,  $t_{\text{rej}} < t_0$ . This implies that this strong rejuvenation is confined to the regime  $\omega t_w < 1$ , which is out of reach for measurements of the ac susceptibility (note that strong rejuvenation is not always observed experimentally in the real part of the susceptibility<sup>10</sup>).

In agreement with Ref. 26, the relaxing curve after the temperature drop is independent of  $t_s$  on the explored range ( $t_s = 10^6, 2 \times 10^7$ , and  $2 \times 10^8$  MCSs in  $D=3$ ). Also shown in Fig. 1 is the relaxation of  $\chi(\omega, t_w)$  for a direct quench to  $T_2$  (dashed line). Such an infinitely fast temperature drop is not realistic (see Sec. III B). Anyhow, the relaxation is not identical to the one after the temperature shift, but the two become very similar (in  $D=3$ , this happens for  $t_w \sim 4t_0$ ). This is in marked contrast with previous simulations where  $t_s \sim 10^4$  and  $t_0=64$ .<sup>9</sup> For such short times, one needs  $t_w \sim 500t_0$  for the two relaxation curves to approach each other.

Yet, in Fig. 1 we assumed to be in pseudoequilibrium regime. In order to estimate the FDT correction factor  $X[C]$  we use the following procedure. We stay for time  $t_s$  at  $T_1$ , then change temperature to  $T_2$ , wait for time  $t_w$  and switch on a small uniform magnetic field ( $h=0.03$ ). We then record the magnetization,  $m(t_w+t)$ , and  $C(t_w, t_w+t)$ . The sought  $X[C]$  factor is obtained drawing  $\chi T = m(t+t_w)T/h$  vs  $C(t_w, t_w+t)$  (insets of Fig. 2). The resulting plot,  $t_w$  independent for large  $t_w$ ,<sup>36</sup> can be fitted with two straight lines, yielding  $X[C]$ . In Fig. 2 (top) we show the time evolution of the  $\chi(\omega, t_w)$  for the same cycle as Fig. 1 with  $t_s=2 \times 10^7$ . Correcting with  $X[C]$  reduces rejuvenation to the point that *strong rejuvena-*

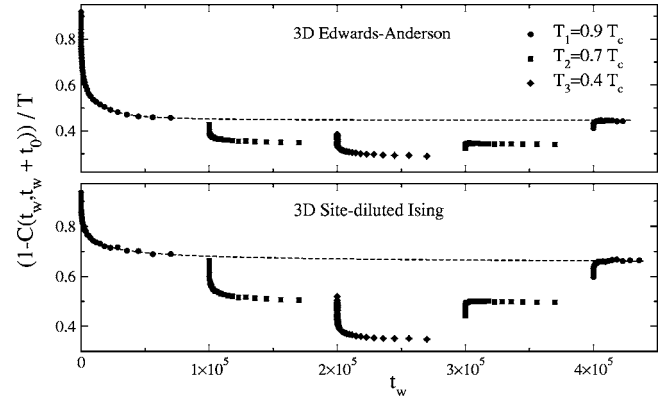


FIG. 3. Naive susceptibility in a three-temperature protocol (see text for details), for the binary EA  $D=3$  model (top) and the  $D=3$  site diluted ferromagnetic Ising model (bottom). The dashed line is a direct quench to  $T_1$ .

tion is no longer seen. The susceptibility no more grows at the temperature drop to  $T_2$ , although the relaxation restarts and still collapses appreciably with the  $\chi(\omega, t_w)$  curve obtained from a direct quench. Similar conclusions are drawn in four dimensions.<sup>39</sup> We report in Fig. 2 (bottom) results for a cycle with a smaller temperature step ( $T_1=0.9T_c$ ,  $T_2=0.7T_c$ ). Here, (see inset), we stay in the pseudoequilibrium regime and rejuvenation is *stronger* for the smaller temperature drop, once the correcting  $X[C]$  factor is considered. However, the collapse with the direct-quench curve starts only for  $t_w \sim 20t_0$ .

### 1. Diluted ferromagnet

Memory and rejuvenation have been found in systems other than spin glasses. A disordered ferromagnetic alloy,<sup>16</sup> becoming spin glass at lower temperatures, has shown rejuvenation but much weaker memory, through the dip-experiment protocol. For comparison, we have simulated a site-diluted Ising model for  $p=0.395$  ( $T_c$  is accurately known<sup>37</sup>). All the interactions being ferromagnetic, there is no temperature chaos in this system. We have simulated a  $L=100$  system checking that  $\xi_T \ll L$  in our simulation window. We measure the naive susceptibility with the autocorrelation function (6). Just for fun, we try a three-step protocol,  $T_1=0.9T_c \rightarrow T_2=0.7T_c \rightarrow T_3=0.4T_c \rightarrow T_2 \rightarrow T_3$ , staying  $t_s = 10^5$  MCSs at each temperature. The results are shown in Fig. 3 (bottom) together with the results for an equal protocol for the 3D EA model (Fig. 3, top). In both cases rejuvenation and a *double* memory are observed. Also in two temperature cycles<sup>39</sup> the susceptibility behaves as in the EA model. To this level of analysis, there is no clear difference between the Edwards-Anderson model and the site-diluted Ising model.

### B. Comparison with experimental direct quench

In view of Eqs. (1) and (2), and the large temperature drop that we are studying, one would expect a perfect rejuvenation effect. However, Figs. 1 and 2 show that the relaxation after the first step at  $0.9T_c$  considerably differs from the direct quench (although this difference is smaller than for

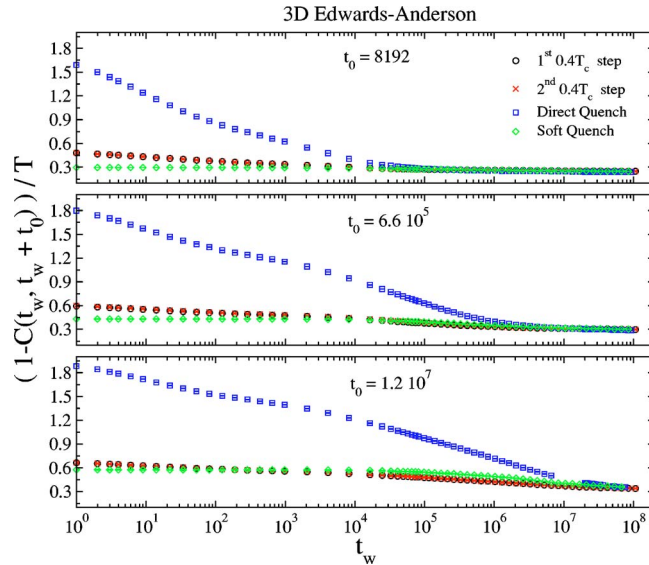


FIG. 4. (Color online) Naive  $\chi(\omega=2\pi/t_0, t_w)$  of the 3D EA model vs time, at temperature  $T_2=0.4T_c$ , for several values of  $t_0$  and thermal histories. In all cases,  $t_w$  is measured from the time of the (last) instantaneous quench to  $T_2$ . Squares correspond to the instantaneous drop from infinite temperature to  $T_2$ . Circles correspond to the system that has spent  $t_s=2 \times 10^8$  MCSs at  $T_1=0.9T_c$ , then suffers an instantaneous quench to  $T_2$ . Crosses correspond to the system that has been a time  $t_s$  at  $T_1$ , then time  $t_s$  at  $T_2$ , then time  $t_s$  at  $T_1$ , and finally suffers the instantaneous quench to  $T_2$ . Diamonds correspond to a gradual drop from  $9T_c$  to  $T_2$  in 20 000 MCSs (we incremented  $1/T$  in  $0.113/T_c$  every  $10^3$  steps, the system spending  $1.2 \times 10^4$  MCSs in the spin-glass phase).

shorter simulations<sup>9,24</sup>). This seems in plain contradiction with experiments (see, e.g., Fig. 4 of Ref. 18). Yet, upon reflection, one realizes that the experimental direct quench bears little resemblance with the simulational one. In fact, the experimental sample that is “instantaneously” quenched to  $0.4T_c$ , spends at least 10 sec ( $\sim 10^{13}$  MCSs!) in the spin-glass phase.

In order to make a fair comparison with experiments, one should study the relaxation after a “soft” quench (Fig. 4) from high temperature to the working temperature below the glass transition. Yet, the fastest quenching rate that can be achieved in experiments is far too slow to be reproduced in present-day computers. To achieve a very slow temperature drop from high temperature to working temperature, it is useful to consider Fig. 1 in a different way. One realizes that the system that has spent  $t_s=2 \times 10^8$  MCSs at  $0.9T_c$ , then suffers an instantaneous temperature drop to  $0.4T_c$ , is a better approximation to the experimental direct quench to  $0.4T_c$ . In fact, the system spends quite a long time close to the critical temperature, where the time evolution—recall Eq. (3)—is faster. When looking to the double temperature cycle in Fig. 1, one needs to compare the relaxation in the first and in the second steps at  $0.4T_c$ , the first corresponding to the *reference* direct quench, the second being looked at as the *temperature-cycled* system. This comparison is shown in Fig. 4, together with the relaxation after a *soft quench*.

The frequencies shown in Fig. 4 span three orders of magnitude. In all cases, the relaxation for the softly quenched

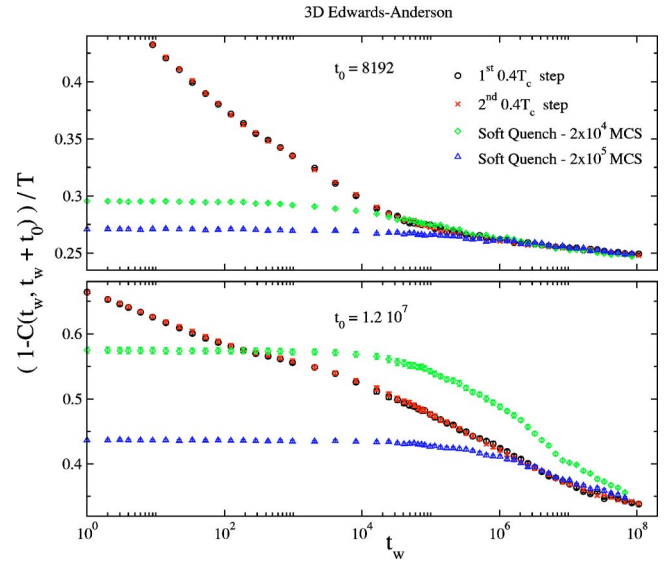


FIG. 5. (Color online) Closeup to the top and bottom panels of Fig. 4, excluding the data for the instantaneous drop from infinite temperature to  $T_2=0.4T_c$ . We also include data (triangles) for a still slower drop from  $9T_c$  to  $T_2$  in 200 000 MCSs (we incremented  $1/T$  in  $0.113/T_c$  every  $10^4$  steps, so that the system spends  $1.2 \times 10^5$  MCSs in the spin-glass phase).

system,<sup>40</sup> that has spent  $1.2 \times 10^4$  MCSs in the spin-glass phase, is much closer to the one of the cycled system than the one of infinite quenching rate. Furthermore, the relaxations for the first and the second steps at  $0.4T_c$  are identical, up to our statistical accuracy (see Fig. 5). This you may wish to call *perfect rejuvenation*.

In Fig. 5 we perform a detailed comparison between the soft quench (with two quenching rates) and the two-step protocol. To have a feeling of the frequency dependence, we show the smallest and the largest frequencies in Fig. 4. For very short times, in the two-step protocols we find a quick decay of the susceptibility due to the sharp temperature drop. On the other hand, the softly quenched system shows a basically constant behavior (the slower the quench, the lower the initial plateau is). When time becomes of the order of the total time spent in the spin-glass phase during the soft quench, the susceptibility starts to decay and becomes very similar to the two-step protocol. At  $t_0=8192$ , the two soft quenches catch the relaxation of the two-step protocol and become identical. At the smallest frequency, the fastest quench approaches but does not catch the two-step relaxation. On the other hand, for the smallest quenching rate, the relaxation curve becomes identical to the one of the two-step protocol for  $t_w \geq t_0$ , which corresponds to the experimentally accessible time range.

Quite similar results are obtained for the diluted ferromagnet, as we show in Fig. 6. Although it cannot be noticed at the scale of this plot, the relaxations in the first and second temperature step are not identical for the Ising model. They may be made to collapse if the times in the second step are rescaled by a factor of 1.2 (in a protocol  $0.7T_c \rightarrow 0.4T_c \rightarrow 0.7T_c \rightarrow 0.4T_c$ , the needed rescaling factor is 2).

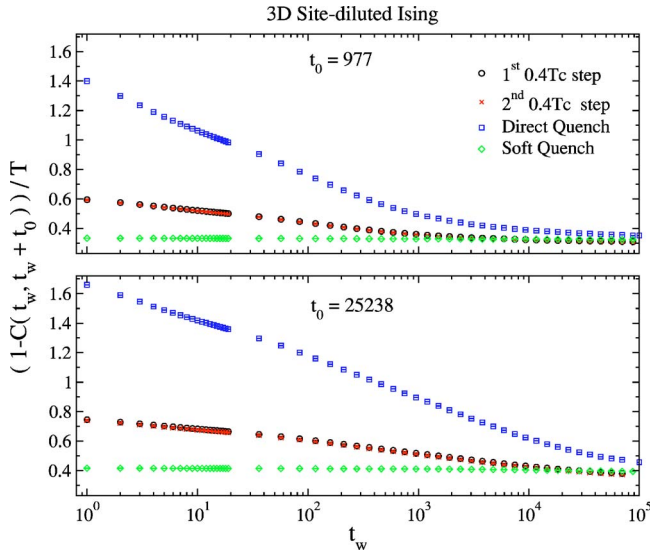


FIG. 6. (Color online) As in Fig. 4, for the diluted ferromagnet and  $t_s = 10^5$  MCSs. Diamonds correspond to a gradual drop from  $9T_c$  to  $T_2$  in 20 000 MCSs (we incremented  $1/T$  in  $0.117/T_c$  every  $10^3$  steps).

### C. Coherence length

The coherence length may play a crucial role<sup>32</sup> in this physics, and should be followed in detail during temperature changes. This was done previously in Ref. 24, for times up to  $10^5$  MCSs. Results in agreement with Eq. (5) were reported. We show here qualitatively different results for our longer simulations in three dimensions.

The coherence length may be obtained from non-self-averaging integrals of  $C_4(r, t_w)$  using a second-momentum estimator.<sup>41,42</sup> Not having so many samples at our disposal, we have obtained  $C_4(r, t_w)$  (which is self-averaging for very large  $r$ ). The resulting curve has been fitted to<sup>29</sup>

$$C_4(r, t_w) = \frac{A}{r^\alpha} \exp\left[-\left(\frac{r}{\xi(t_w)}\right)^\beta\right]. \quad (8)$$

In three dimensions, we find fair fits in the range  $2 < r < 20$ , fixing  $\alpha = 0.65$  and  $\beta = 1.7$  for all times and temperatures. The constant behavior of  $\alpha$  does not agree with the results for the 4D model with Gaussian couplings.<sup>26</sup> To estimate errors in the three-parameter fit (8) is very difficult. To have a feeling of their magnitude, let us report that  $\alpha = 0.7$  yields good fits as well, with a 10% increased  $\xi$  estimate.

See in Fig. 7 (top),  $\xi(t_w)$  for a direct quench to  $T_2 = 0.4T_c$  and for a thermal cycle  $T_1 \rightarrow T_2 \rightarrow T_1$  with  $T_1 = 0.9T_c$  and  $t_s = 2 \times 10^7$ . A power law with exponent  $\sim 0.144$  fits nicely  $\xi_{T_1}(t_w)$  for  $t_w < t_s$ , while the exponent for the direct quench to  $T_2$  is  $\sim 0.065$  (full lines in Fig. 7, top). Note that the exponents follow Eq. (3). During the  $T_2$  step,  $\xi$  grows over the  $T_1$  value, and it is larger than for the direct quench to  $T_2$ . However,  $\xi$  decreases when the system is back to  $T_1$ . Memory is striking: data for the second  $T_1$  step, if translated back  $t_s$  MCSs, are on top of the fit (obtained for  $t_w < t_s$ !). Let us stress two points regarding this result:

(i) The coherence length can *decrease* upon temperature

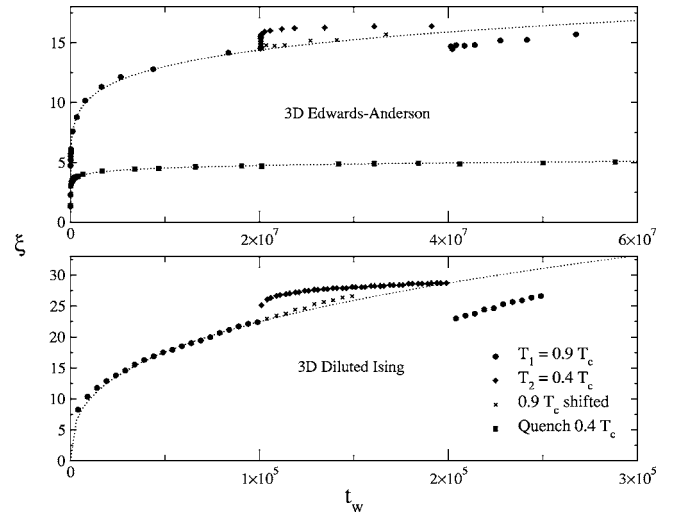


FIG. 7. Coherence length vs time, for the 3D EA model (top) and the diluted-ferromagnet (bottom). The thermal history has been a  $T$  cycle  $T_1 \rightarrow T_2 \rightarrow T_1$ , being  $t_s = 2 \times 10^7$  for the EA model and  $t_s = 10^5$  for the Ising-diluted model. Crosses: second  $T_1$ -step data, translated back in time  $t_s$ ; dotted lines: fits to  $\xi(t_w) = At_w^x$  for  $t_w < t_s$ .

changes, violating cumulative aging, Eq. (5), and in contradiction with the time and length scales separation scenario.<sup>32,43</sup> However, the effect is not symmetrical for negative and positive temperature shifts, as it was inferred experimentally from effective-time measurements.<sup>17</sup>

(ii) The effective time for the temperature cycle is compatible with zero (within our accuracy). This implies that, for  $t_s \sim 10^7$ ,  $x_0$  in Eq. (1) is *not* of order 1, as it was found<sup>27</sup> for  $t_s \sim 10^4$ .

As before (bottom part of Fig. 7), the behavior of the diluted ferromagnet is completely analogous to the one of the EA model [including the power-law growth of  $\xi_T(t)$ ].

### D. Coherence length and two-time correlations

A rather crucial feature of aging<sup>2</sup> is that two time scales,  $t_0$  and  $t_w$ , are involved. One would like to relate the *one*-time quantity  $\xi_T(t_w)$ , to the *two*-time correlation function. A crude estimate for  $t_0 \gg t_w$  is

$$C(t_w, t_w + t_0) \propto \frac{\xi^{D/2}(t_w)}{\xi^{D/2}(t_w + t_0)}, \quad (9)$$

i.e., the coherent cluster that at time  $t_w + t_0$  has linear size  $\xi(t_w + t_0)$ , at time  $t_w$  was composed of mutually incoherent clusters of linear size  $\xi(t_w)$ .

Indeed (Fig. 8, top), the factor  $\xi^{3/2}(t_w + t_0) / \xi^{3/2}(t_w)$  absorbs almost all the  $t_w$  and  $t_0$  dependency of  $C(t_w, t_w + t_0)$ , both for a direct quench to  $T_2$  and for the  $T_2$  part of the thermal cycle. Note that even the constant value for  $C(t_w, t_w + t_0) \xi^{3/2}(t_w + t_0) / \xi^{3/2}(t_w)$  is equal for the direct quench and for the thermal cycle. Also at  $T_1$ ,  $C(t_w, t_w + t_0) \xi^{3/2}(t_w + t_0) / \xi^{3/2}(t_w)$  is constant within a band of width 5% of its mean value.<sup>39</sup> Quite similar results are obtained for the diluted ferromagnet, as we show in the bottom part of Fig. 8. In spite of the crudeness of the argument leading to Eq. (9) and the uncertainty in the

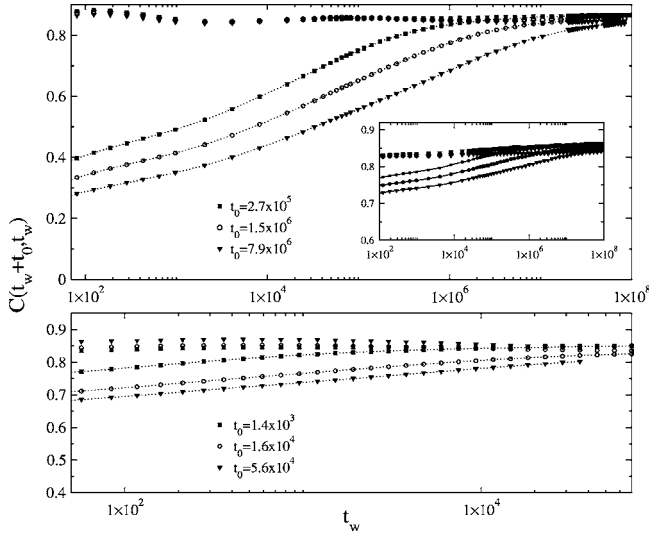


FIG. 8. Top:  $C(t_w, t_w + t_0)[\xi(t_0 + t_w)/\xi(t_w)]^{3/2}$  (points) and  $C(t_w, t_w + t_0)$  (lines) vs  $t_w$ , for the direct quench to  $T_2$ , for the EA model in three-dimensions. Inset: As main plot for the  $T_2$  step of the  $T$  cycle of Fig. 1. Bottom: As inset of top panel for the diluted Ising model.

determination of  $\xi$ , the results are surprisingly clear.

Note that if Eq. (9) was *exact* the dynamics would be of the one-sector type,<sup>2</sup> which we do *not* believe to be the case.<sup>44</sup> Anyhow, given Eq. (9), full aging<sup>4</sup> is natural for a power-law growth of  $\xi(t_w)$ .

Thus memory and rejuvenation are driven by the rate growth of  $\xi_T(t_w)$  rather than by its value or by the short-distance behavior of  $C_4(r, t_w)$ .<sup>32,26</sup> In our simulation, rejuvenation is due to a *growth* of  $\xi$  upon cooling (probably because of a sudden fall into a nearby energy minima), provoking a change in the evolution of  $C(t_w, t_w + t_0)$ . When temperature is shifted back to  $T_1$ ,  $\xi_{T_1}$  continues its growth as if it had never being at  $T_2$  with analogous consequences for the correlation function (memory). This implies a nonmonotonic behavior of  $\xi_T(t)$ , in contradiction with cumulative aging, Eqs. (4) and (5).

### E. Results for $\omega t_w < 1$

Measurements of ac susceptibility are usually confined to the region  $\omega t_w > 1$ . On the other hand, thermal magnetoresistance measurements can yield information on the time regime  $t_0 \gg t_w$ . It is therefore worthwhile to have a look to our correlation functions in this regime.

The main issue here is the characterization of the time decay of correlations (see Ref. 44 for a recent study). One finds<sup>2</sup> that, at least when the correlation function lies in some intervals [say  $C_1 < C(t_w, t_w + t_0) < C_2$ ], it behaves as a function of  $t_0/t_w^\mu$ . It is possible that different intervals for the correlation functions (usually called *time sectors*<sup>2</sup>) are ruled by different exponents. The existence of more than one time sector is a necessary (but not sufficient) requirement for dynamic ultrametricity.<sup>2</sup> Some indications of the presence of more than one time sector in the dynamics of the EA model in three-dimensions were found in Ref. 44.

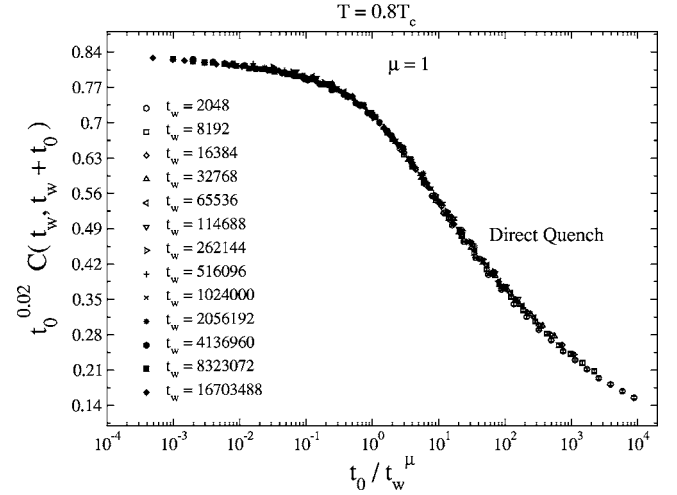


FIG. 9. Correlation function  $C(t_w, t_w + t_0)$  scaled by  $t_0^{0.02}$  [see Eq. (10)] after a direct quench to  $T = 0.8T_c$  vs  $t_0/t_w^\mu$ .

The experimental value of  $\mu$  is controversial. Recently,<sup>4</sup> it was claimed that it is  $\mu = 1$  (full aging). Previous failures in recognizing this were ascribed to quenching-rate effects<sup>4</sup> (recall also Sec. III B). In the quickest possible quench,  $\mu = 1$  was clearly identified. This interpretation was recently disputed by the Saclay group,<sup>5</sup> that find  $\mu < 1$ .

Regarding computer simulations, the following scaling form for the time-correlation function was proposed,<sup>45</sup> and found to work for a restricted  $t_0$  and  $t_w$  range:

$$C(t_w, t_w + t_0) = t_0^{-x(T)} \Phi\left(\frac{t_0}{t_w}\right). \quad (10)$$

This equation implies that full aging should be observed in the  $t_0 \gg t_w$  regime. More recent and longer simulations<sup>44</sup> found deviations from Eq. (10), at least at some temperatures.

In Fig. 9 we plot our data for a direct quench from infinite temperature to  $0.8T_c$ . Equation (10) works nicely with  $x(T) = 0.02$ , which can be interpreted as evidence for full-aging behavior. However, at  $T = 0.4T_c$  (see Fig. 10), we have been unable to find a working  $x(T)$ . Actually, the relaxation is better interpreted in terms of two time sectors: for  $t_0 \gg t_w$ ,  $\mu = 1$  seems to provide a proper scaling, while, at shorter  $t_0$ ,  $\mu = 2/3$  does a better job.

In the inset of 1, we compare the relaxations at  $T = 0.4T_c$  for the direct quench and for the system that stayed  $2 \times 10^8$  MCSs at  $0.9T_c$ , then suffers a temperature shift to  $0.4T_c$  (recall that this is our slowest quenching rate from infinite temperature). For the slowly quenched system, the relaxation belongs to the  $\mu = 2/3$  time sector. Moreover, the relaxation after the  $T$  shift provides a limiting curve, in the large  $t_w$  limit, for the  $\mu = 2/3$  piece of the direct-quench relaxation.

At least within the time range that we can study, it seems that the quenching rate does exert influence in the measured value of  $\mu$  (as proposed in Ref. 4).

## IV. CONCLUSIONS

In this work, we have compared memory and rejuvenation effects for the  $D = 3$  and  $D = 4$  binary EA model and for the

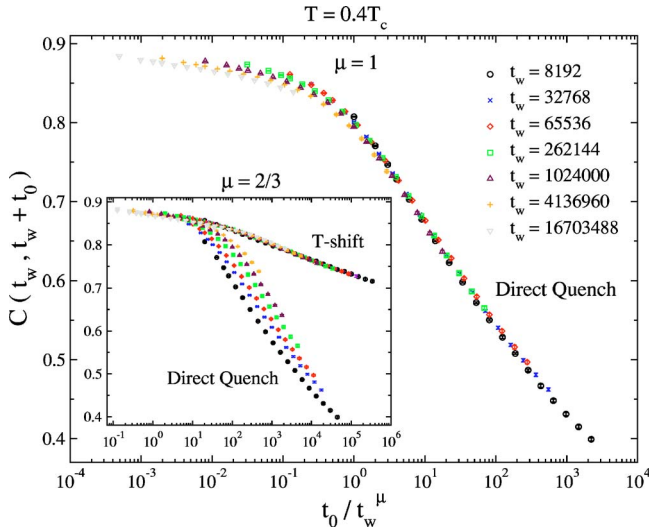


FIG. 10. (Color online) Correlation function  $C(t_w, t_w + t_0)$  after a direct quench to  $T=0.4T_c$  vs  $t_0/t_w^\mu$ . Inset: Data of main plot vs  $t/t_w^\mu$ ,  $\mu=2/3$ . We also plot data for a system that has been  $2 \times 10^8$  MCSs at  $0.9T_c$ , then suffers a temperature shift to  $0.4T_c$ .

$D=3$  the site-diluted Ising model, finding quite similar results. Maybe the most important question we have addressed is whether the Edwards-Anderson model has a spin-glass low-temperature phase, or not. The longer time scale reachable with the SUE machine<sup>35</sup> (three orders of magnitude longer than previous work), has allowed us to conclude that spin glass behaves like experimental spin glasses in a number of ways:

(i) The relaxation of the ac susceptibility after a large temperature shift is as for a *direct quench*, provided that one does not interpret the term *direct quench* literally in the simulations (Sec. III B). We find little dependency in the previous thermal history, once microscopically short times are neglected.

(ii) Values of  $x_0$ , defined in Eq. (1), are not of order 1 for waiting times  $\sim 10^7$  MCSs (contrary to the finding of Ref. 27 for waiting times of order  $\sim 10^4$  MCSs). This time dependence of  $x_0$  is consistent with the findings in the Migdal-Kadanof lattice.<sup>34</sup>

(iii) The coherence length may *decrease* upon temperature changes, in disagreement with the cumulative aging scenario, and in agreement with recent experiments.<sup>17,18</sup>

(iv) The growth rate of the coherence length rules the decay of the time-correlation function.<sup>28</sup> A very simple formula, Eq. (9), accounts for the behavior of  $C(t_w, t_w + t_0)$  with surprising accuracy, for different temperature protocols. Contrary to the findings of short 4D simulations,<sup>26</sup> we do not find a strong temperature dependency of the replica-field correlation function, Eq. (7), at short distances. We rather ascribe rejuvenation to the coherence length, which rules the long-distance behavior of the correlation function.

(v) The exponent  $\mu$  for the  $t_0/t_w^\mu$  scaling of the decay of

$C(t_w, t_w + t_0)$ , depends on the quenching rate. In agreement with recent experiments,<sup>4</sup> we find that the faster the quench is, the easier it becomes to obtain  $\mu=1$  (see, however, Ref. 5 for experiments contradicting this expectation).

The above findings suggest that the 3D EA model behaves as experimental spin glasses do, contrary to what was inferred from previous shorter simulations.<sup>9,24,25,27</sup> However, there are a few important differences. *First*, the out-of-phase and the in-phase susceptibility behave quite differently in experimental spin glasses (see, e.g., Ref. 10). This seems not to be the case for the EA model,<sup>9,27,39</sup> within the accessible time window. *Second*, the coherence length is not found to decrease under positive temperature shifts, in contradiction with the inferred behavior from experimental measurements of effective times.<sup>17,18</sup> *Third*, in the dip-experiment protocol we have found<sup>39</sup> no memory and very weak rejuvenation, in agreement with Ref. 25 even if we study frequencies 15 times smaller. *Fourth*, recent simulations do not<sup>27,46</sup> find stronger memory and rejuvenation effects for Heisenberg than for Ising models of spin glasses. This finding is in contradiction both with experiments (see, e.g., Ref. 19) and with a recent calculation of overlap lengths in the Migdal-Kadanoff approximation.<sup>47</sup> The physical reasons underlying these differences between our best model for spin glasses and experimental spin glasses are not yet understood. It is of course possible that longer times need to be studied. However, when time scales are converted to length scales, one finds that numerical coherence lengths are smaller than the experimental ones only by a small factor (see also Ref. 48).

We have shown that the ferromagnetic site-diluted Ising model (where chaos is absent) follows very closely the behavior of the EA model, at least in the  $\omega t_w > 1$  regime. This is not totally unexpected, as we already know experimentally that systems quite different from spin glasses show memory and rejuvenation.<sup>12-16</sup> The natural conclusion is that chaos, although probably present in realistic spin glasses,<sup>34,38,47</sup> need not be invoked to explain memory and rejuvenation. However, it has been argued<sup>11</sup> that the experimental protocol introduced in Ref. 17 may help to discriminate temperature chaos from a somehow trivial restarting of the dynamics (yet, see Ref. 49). More work will be needed to assess the usefulness of this interesting classification<sup>11</sup> of aging systems.

## ACKNOWLEDGMENTS

We thank G. Parisi, A. Taranc3n, L. A. Fern3ndez, F. Ricci-Tersenghi, E. Marinari, and A. Maiorano for discussions. Numerical simulations have been carried out in the dedicated computer SUE and in the PC clusters *RTN3* and *RTN4*, of U. de Zaragoza. S.J. and S.P.-G. acknowledge financial support from DGA (Spain) and (S.J.) from the ECHP program, Contract No. HPRN-CT-2002-00307, DYGLAGE-MEM. This work has been financially supported by MEC (Spain) through research Contract Nos. FPA2000-0956, FPA2001-1813, BFM2003-08532, and FIS2004-05073-C04.

- <sup>1</sup>See, e.g., *Spin Glasses and Random Fields*, edited by A. P. Young (World Scientific, Singapore, 1997).
- <sup>2</sup>J. P. Bouchaud, L. Cugliandolo, J. Kurchan, and M. Mézard, in *Spin Glasses and Random Fields* (Ref. 1); J. J. Ruiz-Lorenzo *Advances in Condensed Matter and Statistical Mechanics*, edited by E. Korutcheva and R. Cuerno (Nova Science Publishers, 2004).
- <sup>3</sup>R. V. Chamberlin, M. Hardiman, and R. Orbach, *J. Appl. Phys.* **52**, 1771 (1983); L. Lundgren, P. Svedlindh, P. Nordblad, and O. Beckman, *Phys. Rev. Lett.* **51**, 911 (1983); *J. Appl. Phys.* **57**, 3371 (1985).
- <sup>4</sup>At least for  $10^{-2} < t/t_w < 10^2$ ; G. F. Rodriguez, G. G. Kenning, and R. Orbach, *Phys. Rev. Lett.* **91**, 037203 (2003).
- <sup>5</sup>V. Dupuis, F. Bert, J.-P. Bouchaud, J. Hammann, F. Ladieu, D. Parker, and E. Vincent, cond-mat/0406721.
- <sup>6</sup>The ZFC magnetization is a function of  $t/t_w^\mu$ ,  $t$  being measured from the instant when the magnetic field was switched on.
- <sup>7</sup>K. Jonason, E. Vincent, J. Hammann, J. P. Bouchaud, and P. Nordblad, *Phys. Rev. Lett.* **81**, 3243 (1998).
- <sup>8</sup>L. Lundgren, P. Svedlindh, and O. Beckman, *J. Magn. Magn. Mater.* **31-34**, 1349 (1983); T. Jonsson, K. Jonason, P. Jönsson, and P. Nordblad, *Phys. Rev. B* **59**, 8770 (1999); J. Hammann, E. Vincent, V. Dupuis, M. Alba, M. Ocio, and J.-P. Bouchaud, *J. Phys. Soc. Jpn.* **69**, 206 Suppl. A, (2000).
- <sup>9</sup>H. Takayama and K. Hukushima, *J. Phys. Soc. Jpn.* **71**, 3003 (2002).
- <sup>10</sup>S. Miyashita and E. Vincent, *Eur. Phys. J. B* **22**, 203 (2001).
- <sup>11</sup>P. E. Jönsson, H. Yoshino, H. Mamiya, and H. Takayama, *Phys. Rev. B* **71**, 104404 (2005).
- <sup>12</sup>H. Yardimci and R. L. Leheny, *Europhys. Lett.* **62**, 203 (2003).
- <sup>13</sup>L. Bellon, S. Ciliberto, and C. Laroche, *Eur. Phys. J. B* **25**, 223 (2002).
- <sup>14</sup>K. Fukao and A. Sakamoto, cond-mat/0410602.
- <sup>15</sup>P. Levy, F. Parisi, L. Granja, E. Indelicato, and G. Polla, *Phys. Rev. Lett.* **89**, 137001 (2002).
- <sup>16</sup>E. Vincent, V. Dupuis, M. Alba, J. Hammann, and J.-P. Bouchaud, *Europhys. Lett.* **50**, 674 (2000).
- <sup>17</sup>P. E. Jönsson, H. Yoshino, and P. Nordblad, *Phys. Rev. Lett.* **89**, 97201 (2002).
- <sup>18</sup>P. E. Jönsson, R. Mathieu, P. Nordblad, H. Yoshino, H. A. Katori, and A. Ito, *Phys. Rev. B* **70**, 174402 (2004).
- <sup>19</sup>F. Bert, V. Dupuis, E. Vincent, J. Hammann, and J.-P. Bouchaud, *Phys. Rev. Lett.* **92**, 167203 (2004).
- <sup>20</sup>That is, one ages the system at  $T_2$  for time  $t_{T_2}^{\text{eff,shift}}$ , then switches on the magnetic field and records the growing magnetization.
- <sup>21</sup>We somehow simplify the protocol description; for details see Ref. 19.
- <sup>22</sup>The actual value of  $x_0$  depends both on  $T_1$  and on the anisotropy of the microscopic spin-spin interaction [the more Heisenberg-like the interaction is, the smaller  $x_0$  becomes (Ref. 19)].
- <sup>23</sup>J.-P. Bouchaud and D. S. Dean, *J. Phys. I* **5**, 265 (1995); M. Sales, J.-P. Bouchaud, and F. Ritort, *J. Phys. A* **36**, 665 (2003); M. Sasaki, V. Dupuis, J.-P. Bouchaud, and E. Vincent, *Eur. Phys. J. B* **29**, 469 (2002).
- <sup>24</sup>T. Komori, H. Yoshino, and H. Takayama, *J. Phys. Soc. Jpn.* **69**, 228 (2000).
- <sup>25</sup>M. Picco, F. Ricci-Tersenghi, and F. Ritort, *Phys. Rev. B* **63**, 174412 (2001).
- <sup>26</sup>L. Berthier and J.-P. Bouchaud, *Phys. Rev. B* **66**, 054404 (2002).
- <sup>27</sup>A. Maiorano, E. Marinari, and F. Ricci-Tersenghi, cond-mat/0409577.
- <sup>28</sup>See L. W. Bernardi, H. Yoshino, K. Hukushima, H. Takayama, A. Tobo, and A. Ito, *Phys. Rev. Lett.* **86**, 720 (2001), and references therein.
- <sup>29</sup>E. Marinari, G. Parisi, F. Ricci-Tersenghi, and J. J. Ruiz-Lorenzo, *J. Phys. A* **33**, 2373 (2000).
- <sup>30</sup>T. Komori, H. Yoshino, and H. Takayama, *J. Phys. Soc. Jpn.* **68**, 3387 (1999).
- <sup>31</sup>A. J. Bray and M. A. Moore, *Phys. Rev. Lett.* **58**, 57 (1987).
- <sup>32</sup>J. P. Bouchaud, *Soft and Fragile Matter*, edited by M. E. Cates and M. R. Evans (Institute of Physics Publishing, University of Reading, Berkshire, 2000).
- <sup>33</sup>F. Ricci-Tersenghi (private communication).
- <sup>34</sup>M. Sasaki and O. C. Martin, *Phys. Rev. Lett.* **91**, 097201 (2003).
- <sup>35</sup>A. Cruz, J. Pech, A. Tarancón, P. Téllez, C. L. Ullod, and C. Ungil, *Comput. Phys. Commun.* **133**, 165 (2001).
- <sup>36</sup>L. F. Cugliandolo and J. Kurchan, *Phys. Rev. Lett.* **71**, 173 (1993); S. Franz and H. Rieger, *J. Stat. Phys.* **79**, 749 (1995); E. Marinari, G. Parisi, F. Ricci-Tersenghi, and J. J. Ruiz-Lorenzo, *J. Phys. A* **31**, 2611 (1998); D. Hérisson and M. Ocio, *Phys. Rev. Lett.* **88**, 257202 (2002).
- <sup>37</sup>H. G. Ballesteros, L. A. Fernández, V. Martín-Mayor, A. Muñoz Sudupe, G. Parisi, and J. J. Ruiz-Lorenzo, *Phys. Rev. B* **58**, 2740 (1998).
- <sup>38</sup>T. Rizzo and A. Crisanti, *Phys. Rev. Lett.* **90**, 137201 (2003).
- <sup>39</sup>S. Jiménez, Ph.D. thesis, University of Zaragoza, Zaragoza, Spain, 2005.
- <sup>40</sup>Soft quench in this context actually means not infinite quenching rate, but dramatically faster than in experiments.
- <sup>41</sup>F. Cooper, B. Freedman, and D. Preston, *Nucl. Phys. B* **210**, 210 (1989).
- <sup>42</sup>H. G. Ballesteros, A. Cruz, L. A. Fernández, V. Martín-Mayor, J. Pech, J. J. Ruiz-Lorenzo, A. Tarancón, P. Téllez, C. L. Ullod, and C. Ungil, *Phys. Rev. B* **62**, 14237 (2000).
- <sup>43</sup>Parametrizations of  $C_4(r, t)$  different from Eq. (8) can be found, where  $\xi$  does not decrease; J. P. Bouchaud and L. Berthier (private communication).
- <sup>44</sup>S. Jiménez, V. Martín-Mayor, G. Parisi, and A. Tarancón, *J. Phys. A* **36**, 10755 (2003).
- <sup>45</sup>H. Rieger, *J. Phys. A* **26**, L615 (1993); J. Kisker, L. Santen, M. Schreckenberg, and H. Rieger, *Phys. Rev. B* **53**, 6418 (1996).
- <sup>46</sup>L. Berthier and A. P. Young, *Phys. Rev. B* **71**, 214429 (2005).
- <sup>47</sup>F. Krzakala, *Europhys. Lett.* **66**, 847 (2004).
- <sup>48</sup>K. Hukushima and Y. Iba, cond-mat/0207123.
- <sup>49</sup>L. Berthier and J.-P. Bouchaud, *Phys. Rev. Lett.* **90**, 059701 (2003).